



HAL
open science

Were the synapsids primitively endotherms? A palaeohistological approach using phylogenetic eigenvector maps

Mathieu G. Faure-Brac, Jorge Cubo

► To cite this version:

Mathieu G. Faure-Brac, Jorge Cubo. Were the synapsids primitively endotherms? A palaeohistological approach using phylogenetic eigenvector maps. *Philosophical Transactions of the Royal Society B: Biological Sciences*, 2020, 375 (1793), pp.20190138. 10.1098/rstb.2019.0138 . hal-02447334

HAL Id: hal-02447334

<https://hal.science/hal-02447334>

Submitted on 19 Feb 2021

HAL is a multi-disciplinary open access archive for the deposit and dissemination of scientific research documents, whether they are published or not. The documents may come from teaching and research institutions in France or abroad, or from public or private research centers.

L'archive ouverte pluridisciplinaire **HAL**, est destinée au dépôt et à la diffusion de documents scientifiques de niveau recherche, publiés ou non, émanant des établissements d'enseignement et de recherche français ou étrangers, des laboratoires publics ou privés.

Were the synapsids primitively endotherms? A palaeohistological approach using phylogenetic eigenvector maps

Mathieu G. Faure-Brac¹ and Jorge Cubo^{1*}

¹Sorbonne Université, MNHN, CNRS, Centre de Recherche en Paléontologie - Paris (CR2P), Paris, France

*Corresponding author: jorge.cubo_garcia@upmc.fr

Peer-reviewed research published in: Faure-Brac, M. G., & Cubo, J. (2020). Were the synapsids primitively endotherms? A palaeohistological approach using phylogenetic eigenvector maps. *Philosophical Transactions of the Royal Society B*. 2020;375(1793):20190138. DOI: <https://doi.org/10.1098/rstb.2019.0138>.

The acquisition of mammalian endothermy is poorly constrained both phylogenetically and temporally. Here we inferred the resting metabolic rates (RMR) and the thermometabolic regimes (endothermy or ectothermy) of a sample of eight extinct synapsids using palaeohistology, phylogenetic eigenvector maps, and a sample of seventeen extant tetrapods of known RMR (quantified using respirometry). We inferred high RMR values and an endothermic metabolism for the anomodonts (*Lystrosaurus* sp., *Oudenodon baini*) and low RMR values and an ectothermic metabolism for *Clepsydrops collettii*, *Dimetrodon* sp., *Edaphosaurus boanerges*, *Mycterosaurus* sp., *Ophiacodon uniformis* and *Sphenacodon* sp. A maximum likelihood ancestral states reconstruction of resting metabolic rates performed using the values inferred using phylogenetic eigenvector maps in extinct synapsids, and the values measured using respirometry in extant tetrapods, shows that the nodes Anomodontia and Mammalia were primitively endotherms. Finally, we performed a parsimony optimisation of the presence of endothermy using the results obtained in the present study and those obtained in previous studies that used phylogenetic eigenvector maps. For this, we assigned to each extinct taxa a thermometabolic regime (ectothermy or endothermy) depending on whether the inferred values were significantly higher, lower or not significantly different from the RMR value separating ectotherms from endotherms ($1.5 \text{ mL O}_2 \cdot \text{h}^{-1} \cdot \text{g}^{-0.67}$). According to this optimisation, endothermy arose independently in Archosauromorpha, in Sauropterygia, and in Therapsida.

Keywords: endothermy; synapsids; quantitative paleohistology; paleophysiology

Introduction

One of the greatest challenges of current research in palaeobiology is the inference of physiological features of extinct vertebrates. Among them, endothermy is particularly relevant because this feature is linked to a wide array of anatomical, physiological and behavioural features. Endothermy has been defined as the presence of any mechanism of non-shivering thermogenesis that increases both body temperature and resting metabolic rate (1). Mammals, the only extant synapsids, are endotherms (2–5). The origin of mammalian endothermy is poorly constrained both phylogenetically and temporally, in spite of the fact that the acquisition of this ability is a key innovation (endotherms are less dependent on climatic conditions and can occupy more ecological niches (6)). Many approaches have been used to constrain the phylogenetic and temporal frames of this acquisition. One of them involves identifying unequivocal anatomical correlates of endothermy such as respiratory turbinates or evidence for an insulative pelage (7). Respiratory turbinates are rarely preserved in fossils but bone ridges of turbinate attachment are first recognizable in theriocephalians and in cynodonts (7), so they may have been acquired by the eutheriodonts. Oldest evidence for an insulative pelage (fossilized fur impressions) has been found in the Middle Jurassic nonmammalian therapsids (*Castorocauda lutrasimilis* (Ji, Luo, Yuan et Tabrum, 2006) (8); *Megaconus mammaliaformis* (Zhou, Wu, Martin et Luo, 2013) (9); *Agilodocodon scansorius* (Meng, Ji, Zhang, Liu, Grossnickle et Luo, 2015) (10)). Thermal modelling (11), the isotopic composition of mineralized remains (12) and bone palaeohistology (1,13–15) have also been used to infer the thermophysiology of nonmammalian synapsids. Here we will use this last approach.

Traditionally, qualitative bone histology has been used to estimate the bone growth rate (16–18), indirectly linked to the metabolic rate, i.e. the rate of energy expenditure, and to the thermometabolism (19,20). This framework is based on (A) theoretical grounds “the types of tissue deposited in the bones of extinct animals are the most direct evidence of basal metabolic rates, because they directly reflect growth rates [...]. The sustained deposition of fast-growing bone tissues, as displayed by mammals, birds and other dinosaurs, must reflect sustained high

basal metabolic rates” (21) and (B) empirical evidence: the variation of bone growth rates significantly explained the variation of resting metabolic rates in a sample of extant amniotes (19). More recently, quantitative histology and phylogenetic eigenvector maps (13,22) allowed to infer directly the resting metabolic rates of extinct Archosauromorpha (1,13), Sauropterygia (15) and extinct Therapsida (14). More recently, quantitative histology and phylogenetic eigenvector maps (13,22) allowed to infer directly the resting metabolic rates of extinct Archosauromorpha (1,13), Sauropterygia (15) and extinct Therapsida (14).

Olivier et al. (14) used this last approach and provided evidence for an ancestral acquisition of endothermy at the node Eutherapsida. However, the sample composition of this study (14) did not allow to test the hypothesis of an acquisition of endothermy in a more inclusive node. Thus, the present study is aimed at further constraining the temporal range and the phylogenetic frame of the acquisition of endothermy in Synapsids. To do so, we will infer the metabolic rates of a sample of extinct synapsids (including Carboniferous non-neotherapsid synapsids) using a recently developed bone histological variable, the relative primary osteon area (RPOA) (named previously primary osteon density in 15), and phylogenetic eigenvector maps (PEM) (13,22).

Material and Methods

Material

We analysed femora of a total of 25 species of tetrapods. Seventeen of them are extant tetrapods: three archosaurs (*Gallus gallus* (Linnaeus, 1758), *Anas platyrhynchos* (Linnaeus, 1758) and *Crocodylus niloticus* (Laurenti, 1768)), four lepidosaurs (*Varanus exanthematicus* (Bosc, 1792), *Varanus niloticus* (Linnaeus, 1758), *Podarcis muralis* (Laurenti, 1768) and *Zootoca vivipara* (Lichtenstein, 1823)), three turtles (*Chelodina oblonga* (Gray J.E., 1841), *Pelodiscus sinensis* (Wiegmann, 1835) and *Trachemys scripta* (Thunberg in Schoepff, 1792)), six mammals (*Capreolus capreolus* (Linnaeus, 1758), *Microcebus murinus* (Miller, 1777), *Mus musculus* (Linnaeus, 1758), *Cavia porcellus* (Linnaeus, 1758), *Lepus europaeus* (Pallas, 1778) and *Oryctolagus cuniculus* (Linnaeus, 1758)) and one amphibia (*Pleurodeles waltl* (Michahelles, 1830)), acting as

an outgroup for our analyses.

The remaining eight species are extinct synapsids. The histological thin sections of the Anomodontia (*Lystrosaurus* sp. (Cope, 1870) and *Oudenodon bainii* (Owen, 1860)) analysed were previously studied by Olivier et al. (14). They are the closest relatives of extant mammals in our sample. Both of them come from late Permian and, in the case of *Lystrosaurus*, it can be found until the early Triassic. The other extinct taxa of the sample are older: *Clepsydrops collettii* (Cope, 1875), the oldest known synapsid, and *Ophiacodon uniformis* (Cope, 1878) belong to the Ophiacodontidae clade; *Dimetrodon* sp. (Cope, 1878) and *Sphenacodon* sp. (Marsh, 1878) belong to the Sphenacodontidae clade; *Mycterosaurus* sp. (Williston, 1915) (Varanopidae) and *Edaphosaurus boanerges* (Romer & Price, 1940) (Edaphosauridae). The oldest one, *Clepsydrops collettii*, lived in the Late Carboniferous. The others are Permian taxa. Extinct taxa were chosen primarily because of their availability at the vertebrate hard tissues histological collection of the Museum national d'Histoire naturelle (MNHN, Paris).

Methods

Preparation of sections

Femoral diaphyses were embedded in epoxy resin. Transverse and longitudinal thin sections were obtained and mounted on glass slides (23). These sections were prepared and deposited at the vertebrate hard tissues histological collection of the Paris MNHN, where they are available upon request to the curator (a list of accession numbers is given in supplementary file 1). We studied only the femora because it was the only bone present for all of the extinct taxa analysed. Bone histology was studied through transverse sections, completed, when it was necessary, by longitudinal sections (24). The histological terminology follows (25) with addenda from (26).

Resting metabolic rates

As endothermy cannot be directly inferred from the analysis of bone sections, we used proxies. Metabolic rate is directly linked to the thermometabolism: an endotherm shows a higher metabolic rate than an ectotherm *ceteris paribus* (3). Considering that metabolic rate is linked to

bone growth rate (BGR) and BGR to histological features, then histological features can be used as a proxy to infer metabolic rates (19,20). However, considering that metabolic rate is linked to other functions, as locomotion, digestion, reproduction and regulation, we need to standardise it. For adult endothermic amniotes the basal metabolic rate (BMR) has been defined as the minimum rate of energy expenditure measured under thermoneutral and postabsorptive conditions in the inactive phase of the daily cycle (27). For adult ectothermic amniotes the standard metabolic rate (SMR) has been defined as the minimum rate of energy expenditure measured at a given temperature within the animal's range of activity (28) or as the metabolic rate "measured for fasting individuals during the period of normal inactivity (night for most squamates)" (29). We used the resting metabolic rate (RMR) for the whole sample, defined as the metabolic rate "measured for fasting individuals during the period of normal activity" (29).

RMR, measured in $\text{mL O}_2 \cdot \text{h}^{-1}$, is an indicator of the 'whole' energetic expenditures of the organism. We need to standardise by mass unit. Thus, we used mass-specific RMR, measured in $\text{mL O}_2 \cdot \text{h}^{-1} \cdot \text{g}^{-1}$. The effect of body mass on RMR has been corrected in two different ways in previous studies: (1) the mass-independent RMR measured in $\text{mL O}_2 \cdot \text{h}^{-1} \cdot \text{g}^{-b}$, where 'b' is the allometric exponent of the regression between raw RMR to body mass, and (2) the geometry-corrected RMR measured in $\text{mL O}_2 \cdot \text{h}^{-1} \cdot \text{g}^{-0.67}$, where 0.67 is the allometric exponent of the regression between the ratio surface-to-volume to body mass for geometrically similar organisms (30). We used the geometry-corrected RMR because our sample of extant tetrapods includes growing animals and as a consequence the allometric exponent of the regression between raw RMR to body mass may be a mixture of ontogenetic and interspecific allometry (please see (19) for a detailed discussion on this topic). Thus, we used geometry-corrected RMR ($\text{mL O}_2 \cdot \text{h}^{-1} \cdot \text{g}^{-0.67}$) measured at the ontogenetic stage of sustained high BGR to standardise data and allow repeatability. All RMR values for extant taxa were taken from the literature: most (fourteen) of them come from Montes et al. (19). For the remaining three taxa, values were computed using data taken from other studies: *Capreolus capreolus* from Mauget et al. (31); *Lepus europaeus* from Hackländer et al. (32); and *Oryctolagus cuniculus* from Seltmann

et al. (33).

Quantitative histology

We used a variable strongly correlated with the type of osteogenesis (static versus dynamic) involved in bone formation: relative primary osteon area (RPOA) defined as the ratio between the surface occupied by osteon (S_{osteon}) and the analysed bone surface (S_{total}):

$$RPOA = \frac{S_{\text{osteon}}}{S_{\text{total}}}$$

This variable was proposed previously and named primary osteon density or POD (15). We decided to rename it to avoid confusion with the “primary osteon diameter” defined by (33). Osteon diameter has been shown to be strongly associated with BGR (34). Considering that BGR significantly explains the variation RMR (19), both osteon diameter and osteon density are expected to be associated with RMR. Moreover, high growth rate is very energy consuming (19), so a high value of RPOA is expected to reflect a high RMR. Anyway, in spite of these empirical arguments, we tested the relationship between RPOA and RMR using phylogenetic comparative methods.

Phylogenetic comparative methods Phylogeny

We used phylogenetic comparative methods (PCM) to infer extinct taxa’s RMR. These methods include statistical analyses that take into consideration phylogenetic relationship as an explanatory factor (35). Phylogeny includes topology and branch lengths. In this study, branch lengths are computed as the difference in age between two linked nodes (a more inclusive node and a less inclusive node) or between a node and a terminal taxon. Ages of nodes were taken from the PaleoBiology Data Base (<https://paleobiodb.org> last access: 25th June 2018) and reflect the minimal age of the oldest known fossil included in the clade. A minimal distance of 4 Myr was enforced in cases of nodes having the same age, or a distance of less than 4 Myr.

The phylogeny was taken from previous studies (13,14,36) for extant taxa and the two Anomodontia. The

relationships of other extinct taxa were taken from Brocklehurst et al. (37), except for *Clespydrops collettii* which was placed according to Laurin & de Buffrénil (38). We consider the Archelosauria hypothesis of a close relationship between Testudines and Archosauria, supported by many palaeontological (39,40) and molecular (41) studies.

Phylogenetic Generalised Least Squares (PGLS)

The first step was to test the appropriateness of RPOA as proxy to infer RMR. For this we quantified the fraction of the variation of RMR explained by the variation of RPOA using phylogenetic generalised least squares regressions (PGLS) (42–44) with the caper package (45) in R (46). If a significant fraction of RMR was explained by the variation of RPOA, then this last variable can be confidently used as a predictor to infer the former in a phylogenetic context. Shapiro-Wilk normality test were performed on residuals obtained from the PGLS regression of RMR on RPOA using the ‘shapiro.test’ function from the R core software (46).

Phylogenetic signal

We performed two phylogenetic signal tests (Pagel’s λ (47) and Blomberg’s κ (48)) using the phytools package (49) in R (46).

Phylogenetic Eigenvector Maps (PEM)

The following step was to infer extinct taxa’s RMR, using PEM (22). This method infers quantitative values of a biological variable for target taxa using a model. The topology of the phylogeny is coded as a matrix that is afterwards transformed assuming an evolutionary model and taking into account the quantified values in extant taxa, with the aim of representing trait change patterns. Two parameters control the extent of the evolutionary change along the branches. The a steepness parameter ($0 \leq a \leq 1$) indicates how abrupt are evolutionary changes along branches after each split, whereas the ψ parameter ($0 < \psi < \infty$) indicates the relative evolutionary rate (22,50). We assumed that the trait evolved in a steady

steadily throughout the phylogeny and consistently we assigned a single pair of values (a and ψ), but it is possible to assign specific pairs of parameters to each node in a given phylogeny (22). Under pure Brownian motion (purely neutral evolution), $a = 0$ and the expected changes are proportional to the square root of the branch lengths (22,50). In contrast, when $a = 1$, evolutionary change occurs at a fixed rate d irrespective of branch length (22,50). The a steepness parameter was estimated using the 'PEM.fitSimple' function in *MPSEM* (22) and had a value of 0.353 in the model used to perform inferences. We assigned a default value equal to 1 to the ψ evolutionary rate parameter following Molina-Venegas et al. (50). Considering that a large number of eigenvectors are produced ($n-1$, being n the number of taxa analysed), we used the 'lmforwardsequentialAICc' function in *MPSEM* (22) to perform a forward stepwise selection procedure and compile a set of PEM eigenvectors. Two models are produced, the first one based on the phylogeny only and the second one based on the phylogeny plus a predictor variable (here RPOA). We applied an Akaike Information Criteria (AIC) (51) to find the best model, *i.e.* the one with the highest R square and the lowest AIC value. The chosen model was used to infer target species' RMR using the *MPSEM* package (22) in R (46). Finally, we performed a verification of its accuracy using a in leave-one-out cross-validation test, by re-estimating RMR values of the extant taxa (for which these values are known) using the inference procedure and comparing the empirical values with the inferred ones using the *MPSEM* package (22) in R (46).

Ancestral States Reconstruction

Two ancestral states reconstructions were performed. First, we inferred the maximum likelihood (ML) ancestral states of RMR for all nodes, and the corresponding 95% confidence intervals, using the 'fastAnc' function of the *phytools* package (49) in R (46). Second, we transformed our results of RMR into a dichotomic character: 0 for ectotherms and 1 for endotherms. The threshold to perform this attribution corresponds to a value ($1.500 \text{ mL O}_2 \cdot \text{h}^{-1} \cdot \text{g}^{-0.67}$) slightly lower than the lowest RMR value observed in our sample of extant endotherms. These are *Mus musculus* with 1.697 and *Microcebus murinus* with $1.526 \text{ mL O}_2 \cdot \text{h}^{-1} \cdot \text{g}^{-0.67}$. Thus, a taxon with an inferred

value significantly higher than the threshold is scored as endotherm. This last optimisation was performed using Mesquite software (52), with the "Trace Character History" algorithm, using parsimony.

Results

Quantitative histology

Results from histological quantifications are summarised supplementary file 2.

PGLS

We used PGLS analyses to test whether the explanatory (predictor) variable, here RPOA, explains a significant fraction of the response variable (here RMR). We performed a Shapiro-Wilk normality test on residuals obtained from the PGLS regression of RMR on RPOA and we found that the null hypothesis of normality was rejected ($P=0.001939$). Thus, we performed a natural logarithm transformation of RMR and a natural logarithm transformation of $\text{RPOA}+1$ (because several RPOA values equal zero and the natural logarithm of zero is not defined). We repeated the PGLS regression using the transformed variables and the Shapiro-Wilk test on the residuals did not reject the null hypothesis of normality of residuals ($P=0.3014$). P-value of the PGLS regression between $\ln(\text{RMR})$ on $\ln(\text{RPOA}+1)$ is highly significant ($2.092e^{-06}$). RPOA explains 79% of the variation of RMR ($R^2 = 0.787$; $n = 17$). The highly significant P-value and high R^2 found here allow us to use RPOA as a predictor variable to infer RMR using PEM.

PEM

The first step to perform palaeobiological inferences was the choice of the best model. Two models were tested through an AIC procedure: the first one takes into account the phylogenetic relationships, and a second one adds to it the explanatory (predictor) variable (RPOA). A third possibility (a model including only POD as an explanatory variable; in other words, a model without phylogeny or including a star phylogeny) has been ruled out because both the response variable (RMR) and the explanatory variable (RPOA) show a highly significant phylogenetic signal. Pagel's λ of $\ln(\text{RMR}) = 0.995$, $P=6.577729e-05$; Blomberg's κ of $\ln(\text{RMR}) = 1.396$;

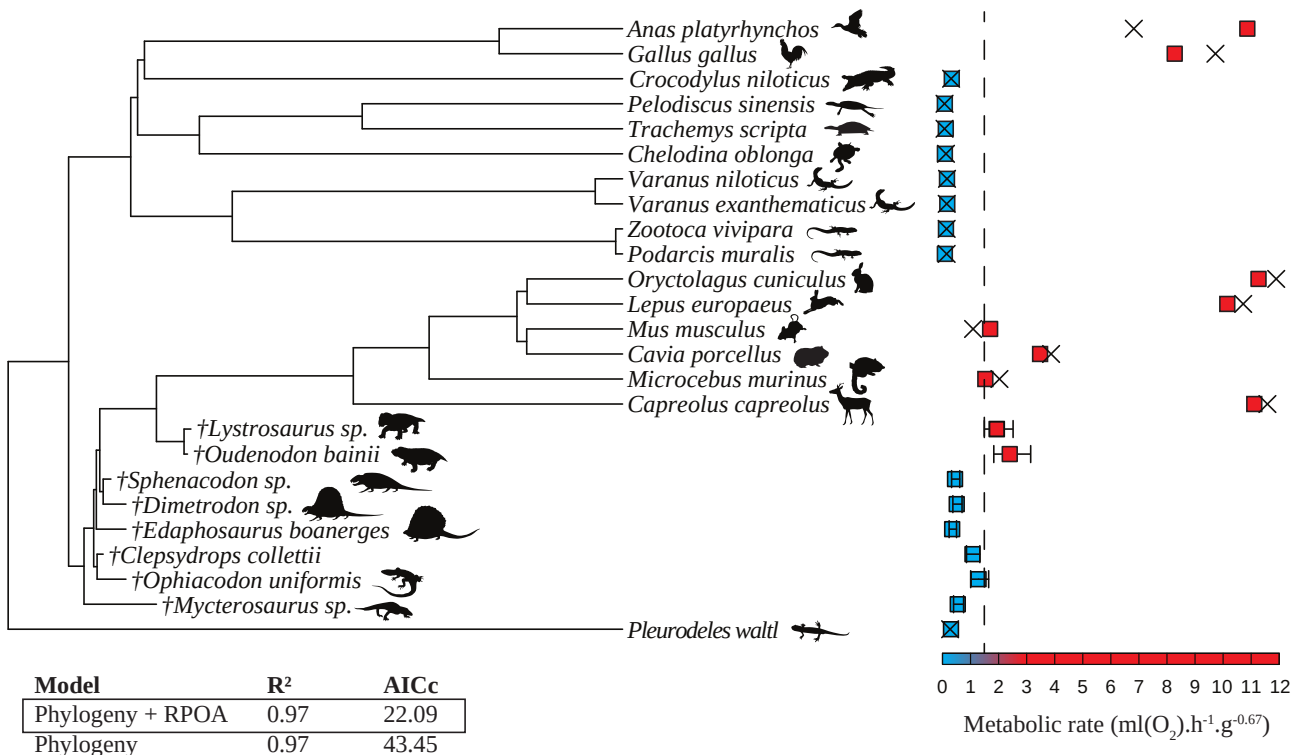


Figure 1. Resting metabolic rates inferred using palaeohistology and phylogenetic eigenvector maps. We used a model that includes the phylogeny plus relative primary osteon area as explanatory factors. Blue squares indicate ectothermy and red squares endothermy. The broken line represents the lower RMR value found in extant endotherms. For extinct taxa, segments represent the 95% confidence intervals of the inferences. For extant taxa, crosses represent values inferred in leave-one-out cross-validation tests.

$P=0.001$. Pagel's λ of $\ln(\text{RPOA}+1) = 0.999$; $P=0.012$; Blomberg's κ of $\ln(\text{RPOA}+1) = 0.613$; $P=0.001$. Results of AIC selection procedure are given in figure 1. The model including RPOA + phylogeny was selected to infer RMR because it shows the highest R squared and the lowest AIC value. Inferred values are shown in figures 1 and 2. Script is provided in supplementary file 3. Our RMR inferences show that the two anomodonts (*Lystrosaurus* sp. and *Oudenodon bainii*) show high RMR values. All these taxa were probably endotherms because the inferred RMR values are significantly higher than the lowest values measured in the extant endotherms of the sample (*Mus musculus* and *Microcebus murinus*). All other extinct taxa show unambiguous ectotherm-like RMR values.

Ancestral States Reconstruction

Maximum likelihood ancestral states reconstructions of RMR using values inferred in this study are shown in figure 2, and a parsimony optimisation of the presence of endothermy using the results obtained in the present study and those obtained in previous studies using PEMs methodology (1,13–15) is shown in figure 3. Of our

our sample of fossil taxa, only value inferred for *Oudenodon* is significantly higher than the threshold separating endotherms from ectotherms ($1.500 \text{ mL O}_2 \cdot \text{h}^{-1} \cdot \text{g}^{-0.67}$). We inferred a high RMR for *Lystrosaurus* ($1.936 \text{ mL O}_2 \cdot \text{h}^{-1} \cdot \text{g}^{-0.67}$), but the inferior limit of the confidence interval is slightly smaller (1.491) than the threshold (1.500). Therefore, we considered that the endothermy of *Lystrosaurus* was marginally significant. Regarding inferences obtained in other studies using PEM, we excluded two taxa in the optimisation of figure 3 because Legendre et al. (13) and Cubo & Jalil (1) found divergent inferred values. These taxa were the archosauriform *Proterosuchus fergusi* (Broom, 1903) and the dinosaur *Maiasaura peeblesorum* (Horner & Makela, 1979).

Discussion

The presence of endothermy in extinct synapsids has been inferred using different proxies. Using proxies is obviously necessary because the thermometabolic regime of extinct taxa is not accessible through direct observation of fossilised features. The presence of anatomical features linked to endothermy in extant mammals, as the presence

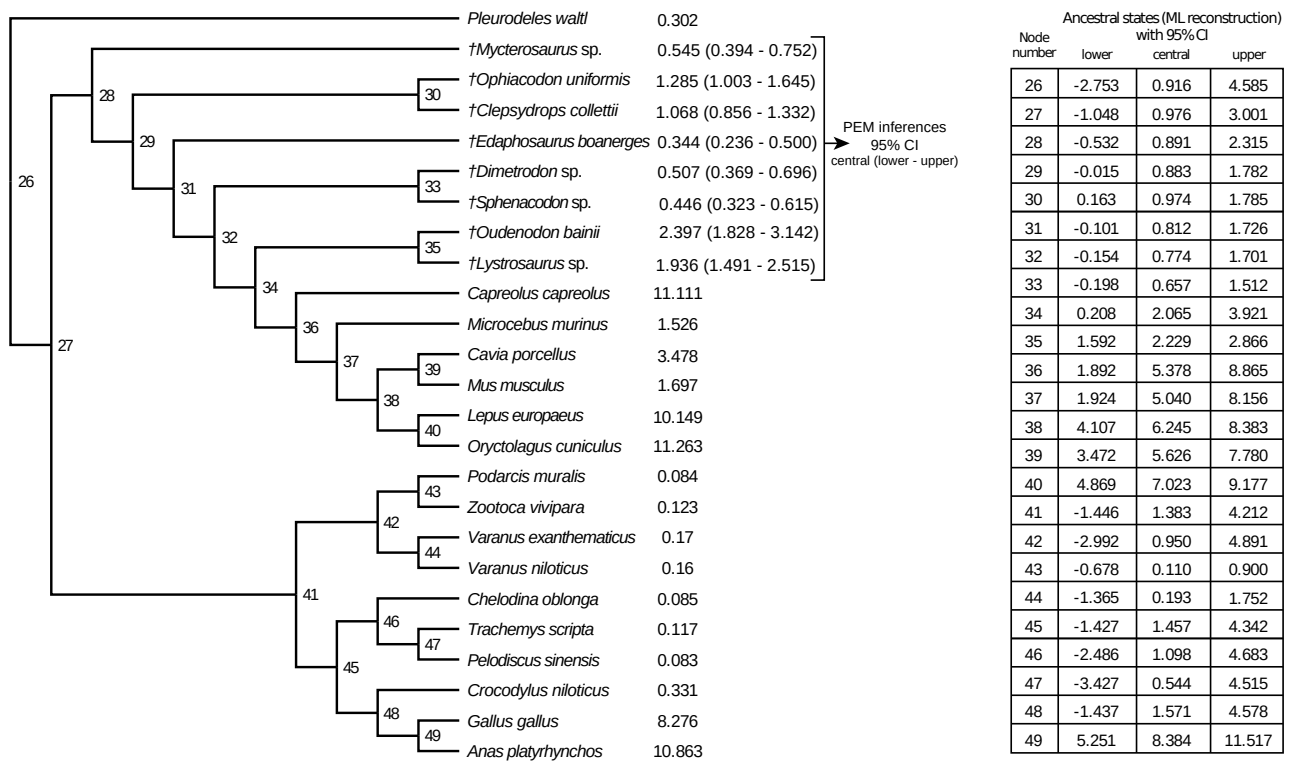


Figure 2. Maximum likelihood ancestral states reconstruction of resting metabolic rates performed using the values inferred using phylogenetic eigenvector maps for the eight extinct synapsids, and the values measured using respirometry in the seventeen extant tetrapods. Within Synapsida, the nodes Anomodontia and Mammalia were primitively endotherms.

of fur (53) or of respiratory turbinates (7) have been widely used. The former has traditionally been seen as evidence for, at least, a near-endothermic condition, because of its homeothermic function by retaining the generated heat (7,53). The earliest known occurrences of fossilized fur impressions have been dated in the Middle Jurassic (*Castorocauda* (8); *Megaconus* (9); *Agilodocodon* (10)). Considering that endothermy has been defined by Cubo & Jalil (1) as the presence of any mechanism of non-shivering thermogenesis (e.g. 5,49,50) that increases both body temperature and resting metabolic rate, the presence of fur and hair are not definitive evidence for endothermy because, at best, they can indicate a homeothermic condition.

The same reasoning can be applied to respiratory turbinates: these are osseous or cartilaginous convoluted pieces in the nasal cavity. The oldest presence of respiratory turbinates in synapsids is dated from Lopingian (late Permian) (56). During inhalation, they warm and moist the incoming air and do the opposite for expiration (56,57). Doing so, they help to keep a stable temperature and limit the loss of moisture through breathing. According to several authors, endothermy cannot be sustained without these structures (58) leading

these to be considered as the best evidence for an endothermic condition. However, the obligate presence of respiratory turbinates to achieve homeothermy was recently challenged (59).

Another proxy is geochemistry. The isotopic ratio between ¹⁶O, the common form of oxygen, and ¹⁸O, a rare heavy isotope, is used to infer body temperature. This ratio, measured in calcium phosphate from bones and, especially, dentary enamel, is dependent on environmental and body temperatures during the formation of the sample (12,60). We can infer the relative internal body temperatures from calcium phosphate using fractionation equations (12,60–63). Lot of studies have been conducted in different organisms, as for Ichthyosaurs and Plesiosaurs (63). Recently, Rey et al. (12) studied a large sample of Neotherapsida with this approach and discussed two competing hypotheses: either a single apparition of endothermy at the Neotherapsida node, or two independent acquisitions at the nodes of Dicynodontioidea and Epicynodontia. According to these results, the endothermy was acquired in the synapsid clade, at best, during the Roadian (early Permian) with the single apparition scenario. With the convergent evolutionary scenario, endothermy would have been appeared during

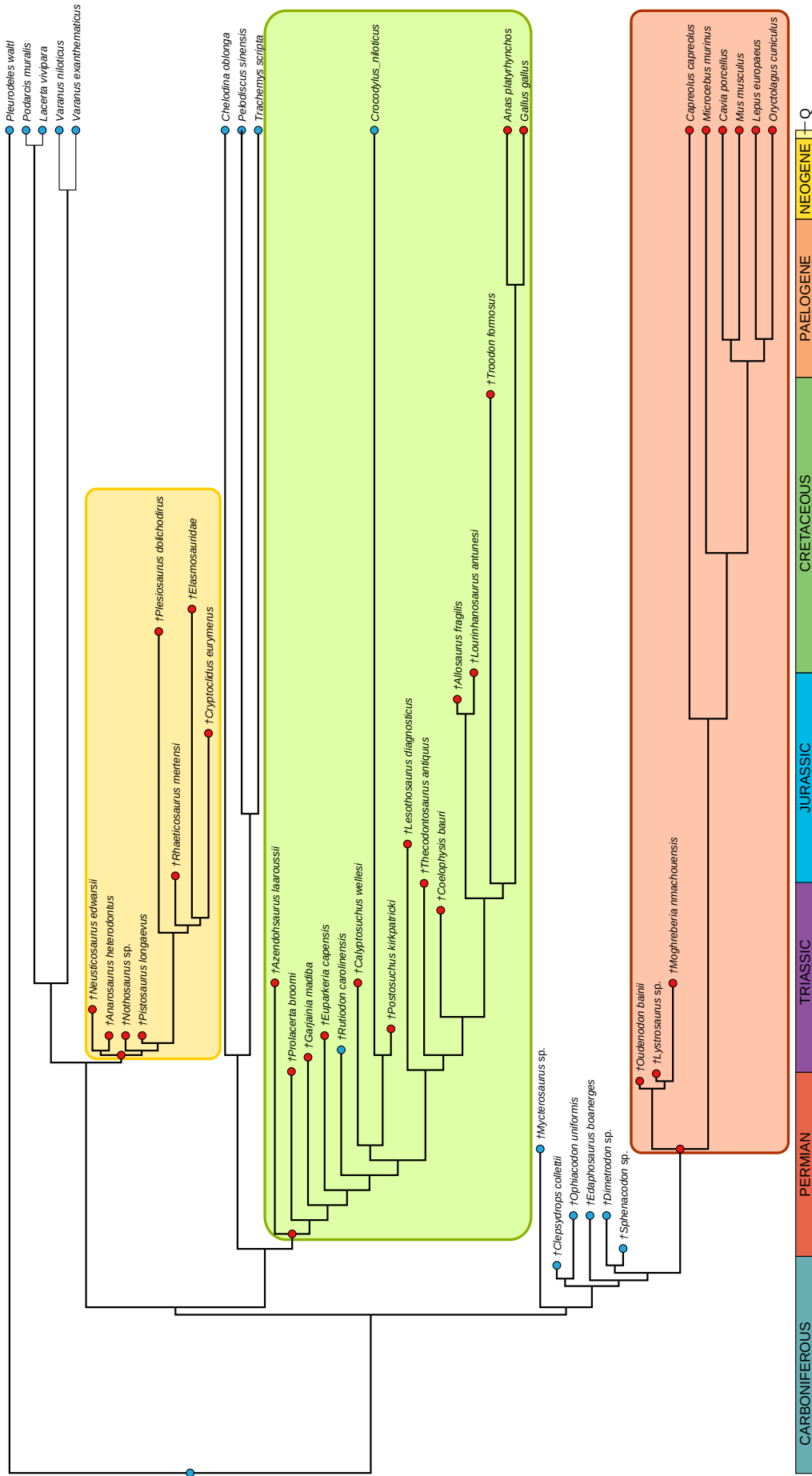


Figure 3. Parsimony optimisation of the presence of endothermy using the results obtained in the present study and those obtained in previous studies using phylogenetic eigenvector maps (1,13–15). For this, we assigned to each extinct taxa a thermometabolic regime (ectothermy or endothermy) depending on whether the inferred values were significantly higher, lower or not significantly different from the RMR value separating ectotherms from endotherms ($1.5 \text{ mL O}_2 \cdot \text{h}^{-1} \cdot \text{g}^{-0.67}$). According to this optimisation endothermy arose independently in Archosauromorpha (green), in Sauropterygia (yellow), and in Therapsida (orange). Blue circles indicate ectothermy and red circles endothermy.

the Lopingian, as for respiratory turbinates.

On the specific case of *Dimetrodon*, some studies tried to estimate the effect of the sail in thermal regulation (11,64). In this specific case, the authors created models in order to simulate the heat exchanges and the specific role of the sail. They concluded that the sail allowed *Dimetrodon* to be active earlier than similar but sail-less predators. However, this proxy deals with external heat income and not with endogenous mechanisms of non-shivering thermogenesis (endothermy).

Bone histology, the last proxy, has largely been based on Amprino's rule (65): the organisation of the collagen matrix records bone growth rate (65). In other words, a fast growth leads to poorly organized type of tissue (*i.e.*, woven bone), whereas a low growth rate produces a highly organized type of tissue (lamellar or non-lamellar parallel fibered bone) (25). Thus the presence of woven bone has been interpreted as evidence for fast bone growth rate, linked to the endothermy (38,66–68). However, many counterexamples exist: many ectotherms, *e.g.*, *Alligator* (69) or *Varanus* (70), are able to form woven bone. In contrast, primary osteon density, the histological feature recently proposed by Fleischle et al. (15), is tightly linked to bone growth rate and to resting metabolic rate. Most endothermic amniotes are able to form an initial scaffold composed of woven bone that includes large cavities and produces a rapid volume expansion of the cortex during early ontogenetic stages (*e.g.* in the long bones of ratites (71) and in the long bones of the king penguin (72)). On the contrary, in most ectothermic amniotes, periosteal bone is composed of parallel-fibered bone including, if any, small cavities, and producing a slow volume expansion of the cortex (*e.g.* in squamates (73)). Consistently, relative primary osteon area (RPOA) was used in this study (primary osteon density in 15; see above) to infer the thermometabolic regime (ectothermic or endothermic) of our sample of extinct synapsids.

RPOA explains a significant fraction of the variation of RMR (quantified using respirometry) in the sample of extant tetrapods (results obtained using PGLS regressions). Thus, assuming the actualism principle, *a priori* the former can be used to infer the later in extinct taxa. Molina-Venegas et al. (50) analysed accuracy of inferences (here retrodictions) using pGLM and PEM approaches. They concluded that accuracy of predictions

is high for traits with high phylogenetic signal (with high Pagel's λ values), and that it decreases when tip branch lengths increases, accuracy being reasonably good for tip branch lengths smaller than 10% of the total length of the tree. In our case study, Pagel's λ for both the response and the explanatory variables are extremely high (Page's $\lambda=0.995$, $P=6.578e-05$ and $\lambda=0.999$, $P=0.012$ respectively) and all tip branch lengths but one (*Mycterosaurus*, see below) are smaller than 10% of the total length of the tree. Therefore we assume that all our RMR inferences obtained using PEM are accurate.

Inferred RMR values for our sample of extinct synapsids using PEM are shown in figures 1 and 2. Value inferred for *Mycterosaurus* should be analysed with caution because the branch length of this taxon (42.3 My) is bigger than 10% of the total height of the tree (358,9 My) and, according to (50), this fact lead to a loss of accuracy when performing inferences. Our inferences for *Lystrosaurus* sp. (1.936 mL O₂ .h⁻¹.g^{-0.67} ; 1.491 - 2.515) and *Oudenodon baini* (2.397 mL O₂ .h⁻¹.g^{-0.67} ; 1.828 - 3.142) are congruent with those obtained by Olivier et al. (14), who used a different histological feature (osteocyte lacunae density). We performed maximum likelihood ancestral states reconstructions using these values and those measured in extant species (figure 2). As expected, RMR inferred for nodes 49 (birds) and 36 (mammals) in figure 2 are significantly higher than the threshold separating endotherms from ectotherms (1.500 mL O₂ .h⁻¹.g^{-0.67}). Likewise, RMR inferred for node 35 (Anomodontia: (*Lystrosaurus* – *Oudenodon*)) is also significantly higher than the quoted threshold. However, value inferred for node 34 (Therapsida:((*Lystrosaurus* – *Oudenodon*) – Mammals))) does not exclude ectothermy. Finally, we performed a parsimony optimisation of the presence of endothermy (figure 3). For this, we assigned to each extinct taxa a thermometabolic regime (ectothermy or endothermy) depending on whether the inferred values were significantly higher, lower or not significantly different from the RMR value separating ectotherms from endotherms (1.500 mL O₂ .h⁻¹.g^{-0.67}). We reconstructed ancestral thermometabolic states (figure 3) using the results obtained in the present study and those obtained in previous studies using PEMs (1,13–15). According to this optimisation (figure 3), endothermy arose three independent times in Amniotes: in Archosauromorpha, in Sauropterygia, and in Therapsida.

The presence of fully developed or incipient endothermy has been suggested in other groups of tetrapods: Ichthyosauria (63,74), Pterosauria (75) and Mososauria (63,76). For both aquatic taxa (mosasaurs and ichthyosaurs) a study using a geochemistry approach suggested a high inner temperature for ichthyosaurs (between 30 and 35°C) and on medium inner temperature for mosasaurs (around 30°C) (63). For ichthyosaurs, this study suggested a fully developed endothermic condition whereas it was probably an incipient endothermy for mosasaurs (57). This result is congruent with that obtained by de Buffrénil and Mazin, who found presence of woven bone suggesting a high growth rate and, so, a high metabolic rate in ichthyosaurs (74). The case of mosasaurs is more complex. Houssaye et al. (76) analysed the bone histology of mosasaurs limb bones and found a predominance of parallel-fibered bone, which doesn't need a high metabolic rate to occur. But they also described unusual parallel-fibered bone, which could reflect a growth rate intermediate between that typical of parallel-fibered bones and that associated to woven bone. The thermometabolic condition of mosasaurs is ambiguous and gigantothermy, a heat conservation linked to high body mass, is not excluded (76). For pterosaurs, de Ricqlès et al. (75) analysed the bone histology of limb bones and found presence of woven bone, especially in juvenile specimens, leading them to the conclusion that these animals had a growth curve similar to those found in extant birds. A high growth rate suggests an endothermic condition for pterosaurs. This condition would be correlated with the presence of air sacs detected in some species (77). Such organs are very important in modern birds to sustain a unidirectional airflow in the lungs and so a high metabolism associated with flight. The finding of unidirectional airflow in the lungs of alligators (78) suggests that this condition would be primitive for archosaurs and so inherited by pterosaurs.

Perspectives. Further research using quantitative histology and PEMs will help to elucidate the thermometabolic condition of ichthyosaurs, pterosaurs, mosasaurs and early synapsids. The predictive power of inference models will increase including additional explanatory factors such as life history traits, as well as new osteohistological features correlated to the thermometabolism, as for instance vascular canals minimum diameter (79).

Acknowledgments

We thank H. Lamrous and S. Morel for preparation of thin sections, D. Germain for access to the hard tissue collection of the French Museum national d'Histoire naturelle and C. Olivier for reading a draft of the paper.

References

1. Cubo J, Jalil N-E. Bone histology of *Azendohsaurus laaroussii*: Implications for the evolution of thermometabolism in Archosauromorpha. *Paleobiology*. 2019;45(2):317–30.
2. Hillenius WJ, Ruben JA. The Evolution of Endothermy in Terrestrial Vertebrates: Who? When? Why? *Physiol Biochem Zool*. 2004 Nov;77(6):1019–42.
3. Clarke A, Pörtner H-O. Temperature, metabolic power and the evolution of endothermy. *Biol Rev*. 2010 Jan 25;85:703–27.
4. Nespolo RE, Bacigalupe LD, Figueroa CC, Koteja P, Opazo JC. Using new tools to solve an old problem: the evolution of endothermy in vertebrates. *Trends Ecol Evol*. 2011 Aug;26(8):414–23.
5. Rowland LA, Bal NC, Periasamy M. The role of skeletal-muscle-based thermogenic mechanisms in vertebrate endothermy: Non-shivering thermogenic mechanisms in evolution. *Biol Rev*. 2015 Nov;90(4):1279–97.
6. Walter I, Seebacher F. Endothermy in birds: underlying molecular mechanisms. *J Exp Biol*. 2009 Aug 1;212(15):2328–36.
7. Ruben JA, Hillenius WJ, Kemp TS, Quick DE. The Evolution of Mammalian Endothermy. In: *Forerunners of Mammals: Radiation, Histology, Biology*. Indiana University Press. Bloomington and Indianapolis: Anusuya Chinsamy-Turan; 2012. p. 273–86.
8. Ji Q, Luo Z-X, Yuan C-X, Tabrum AR. A Swimming Mammaliaform from the Middle Jurassic and Ecomorphological Diversification of Early Mammals. *Science*. 2006 Feb 24;311(5764):1123–7.
9. Zhou C-F, Wu S, Martin T, Luo Z-X. A Jurassic mammaliaform and the earliest mammalian evolutionary adaptations. *Nature*. 2013 Aug;500(7461):163–7.
10. Meng Q-J, Ji Q, Zhang Y-G, Liu D, Grossnickle DM, Luo Z-X. An arboreal docodont from the Jurassic and mammaliaform ecological diversification. *Science*.

- 2015;347(6223):764–8.
- 11 . Florides GA, Kalogirou SA, Tassou SA, Wrobel L. Natural environment and thermal behaviour of *Dimetrodon limbatus*. *J Therm Biol*. 2001 Feb;26(1):15–20.
 - 12 . Rey K, Amiot R, Fourel F, Abdala F, Fluteau F, Jalil N-E, et al. Oxygen isotopes suggest elevated thermometabolism within multiple Permo-Triassic therapsid clades. *eLife* [Internet]. 2017 Jul;6. Available from: <https://elifesciences.org/articles/28589>
 - 13 . Legendre LJ, Guénard G, Botha-Brink J, Cubo J. Palaeohistological Evidence for Ancestral High Metabolic Rate in Archosaurs. *Syst Biol*. 2016 Nov;65(6):989–96.
 - 14 . Olivier C, Houssaye A, Jalil N-E, Cubo J. First palaeohistological inference of resting metabolic rate in an extinct synapsid, *Moghreberia nmachouensis* (Therapsida: Anomodontia). *Biol J Linn Soc*. 2017 Jun 1;121(2):409–19.
 - 15 . Fleischle CV, Wintrich T, Sander PM. Quantitative histological models suggest endothermy in plesiosaurs. *PeerJ*. 2018 Jun 6;6:e4955.
 - 16 . Padian K, de Ricqlès AJ, Horner JR. Dinosaurian growth rates and bird origins. *Nature*. 2001 Jul;412(6845):405–8.
 - 17 . Padian K, Horner JR, De Ricqlès A. Growth in small dinosaurs and pterosaurs: the evolution of archosaurian growth strategies. *J Vertebr Paleontol*. 2004 Sep 10;24(3):555–71.
 - 18 . Botha-Brink J, Smith RMH. Osteohistology of the Triassic archosauromorphs *Prolacerta*, *Proterosuchus*, *Euparkeria*, and *Erythrosuchus* from the Karoo Basin of South Africa. *J Vertebr Paleontol*. 2011 Nov;31(6):1238–54.
 - 19 . Montes L, Le Roy N, Perret M, de Buffrénil V, Castanet J, Cubo J. Relationships between bone growth rate, body mass and resting metabolic rate in growing amniotes: a phylogenetic approach. *Biol J Linn Soc*. 2007 Sep;92(1):63–76.
 - 20 . Montes L, Castanet J, Cubo J. Relationship between bone growth rate and bone tissue organization in amniotes: first test of Amprino's rule in a phylogenetic context. *Anim Biol*. 2010;60(1):25–41.
 - 21 . Padian K, Horner JR. Typology versus transformation in the origin of birds. *Trends Ecol Evol*. 2002 Mar;17(3):120–4.
 - 22 . Guénard G, Legendre P, Peres-Neto P. Phylogenetic eigenvector maps: a framework to model and predict species traits. *Methods Ecol Evol*. 2013 Dec;4(12):1120–31.
 - 23 . Lamm E-T. Preparation and Sectioning of Specimens. In: *Bone histology of fossil tetrapods: advancing methods, analysis, and interpretation*. University of California Press. Berkeley; 2013.
 - 24 . Faure-Brac MG, Pelissier F, Cubo J. The influence of plane of section on the identification of bone tissue types in amniotes with implications for paleophysiological inferences. *J Morphol* [Internet]. 2019 Jun; Available from: <http://doi.wiley.com/10.1002/jmor.21030>
 - 25 . Francillon-Vieillot H, de Buffrénil V, Castanet J, Géraudie J, Meunier FJ, Sire J-Y, et al. Microstructure and Mineralization of Vertebrate Skeletal Tissues. In: *Skeletal biomineralization: patterns, processes and evolutionary trends*. New York: VanNostrand Reinhold; 1990. p. 471–530.
 - 26 . Prondvai E, Stein KHW, de Ricqlès A, Cubo J. Development-based revision of bone tissue classification: the importance of semantics for science: Development-based bone tissue classification. *Biol J Linn Soc*. 2014 Aug;112(4):799–816.
 - 27 . Daan S, Masman D, Groenewold A. Avian basal metabolic rates: their association with body composition and energy expenditure in nature. *Am J Physiol-Regul Integr Comp Physiol*. 1990;259(2):333–40.
 - 28 . Lewis LY, Gatten RE jr. Aerobic metabolism of American alligators, *Alligator mississippiensis*, under standard conditions and during voluntary activity. *Comp Biochem Physiol A*. 1985;80(3):441–7.
 - 29 . Andrews RM, Pough FH. Metabolism of Squamate Reptiles: Allometric and Ecological Relationships. *Physiol Biochem Zool*. 1985;58(2):214–31.
 - 30 . White CR, Seymour RS. Sample size and mass range effects on the allometric exponent of basal metabolic rate. *Comp Biochem Physiol A Mol Integr Physiol*. 2005 Sep;142(1):74–8.
 - 31 . Mauget C, Mauget R, Sempéré A. Energy expenditure in European roe deer fawns during the suckling period and its relationship with maternal reproductive cost. *Can J Zool*. 1999;77(3):389–96.
 - 32 . Hackländer K, Arnold W, Ruf T. Postnatal development and thermoregulation in the precocial European hare (*Lepus europaeus*). *J Comp Physiol [B]*. 2002 Feb 1;172(2):183–90.

- 33 . Seltmann MW, Ruf T, Rödel HG. Effects of body mass and huddling on resting metabolic rates of post-weaned European rabbits under different simulated weather conditions: Resting metabolic rates in juvenile rabbits. *Funct Ecol.* 2009 Dec;23(6):1070–80.
- 34 . de Margerie E, Cubo J, Castanet J. Bone typology and growth rate: testing and quantifying ‘Amprino’s rule’ in the mallard (*Anas platyrhynchos*). *C R Biol.* 2002 Mar;325(3):221–30.
- 35 . Felsenstein J. Phylogenies and the Comparative Method. *Am Nat.* 1985;125(1):1–15.
- 36 . Cubo J, Le Roy N, Martinez-Maza C, Montes L. Paleohistological estimation of bone growth rate in extinct archosaurs. *Paleobiology.* 2012;38(02):335–49.
- 37 . Brocklehurst N, Reisz RR, Fernandez V, Fröbisch J. A Re-Description of ‘*Mycterosaurus*’ *smithae*, an Early Permian Eothyridid, and Its Impact on the Phylogeny of Pelycosaurian-Grade Synapsids. Beatty BL, editor. *PLOS ONE.* 2016 Jun 22;11(6):e0156810.
- 38 . Laurin M, de Buffrénil V. Microstructural features of the femur in early ophiacodontids: A reappraisal of ancestral habitat use and lifestyle of amniotes. *Comptes Rendus Palevol.* 2016 Jan;15(1–2):115–27.
- 39 . Bever GS, Lyson TR, Field DJ, Bhullar B-AS. Evolutionary origin of the turtle skull. *Nature.* 2015 Sep;525(7568):239–42.
- 40 . Schoch RR, Sues H-D. A Middle Triassic stem-turtle and the evolution of the turtle body plan. *Nature.* 2015 Jul;523(7562):584–7.
- 41 . Crawford NG, Parham JF, Sellas AB, Faircloth BC, Glenn TC, Papenfuss TJ, et al. A phylogenomic analysis of turtles. *Mol Phylogenet Evol.* 2015 Feb;83:250–7.
- 42 . Garland T, Ives AR. Using the Past to Predict the Present: Confidence Intervals for Regression Equations in Phylogenetic Comparative Methods. *Am Nat.* 2000;155(3):346–64.
- 43 . Martins EP, Hansen TF. Phylogenies and the Comparative Method: A General Approach to Incorporating Phylogenetic Information into the Analysis of Interspecific Data. *Am Nat.* 1997;149(4):646–67.
- 44 . Grafen A. The Phylogenetic Regression. *Philos Trans R Soc B Biol Sci.* 1989 Dec 21;326(1233):119–57.
- 45 . Orme D. The caper package: comparative analysis of phylogenetics and evolution in R. [Internet]. 2013. Available from: <https://cran.r-project.org/web/packages/caper/vignettes/caper.pdf>
- 46 . R Development Core Team. R: A language and environment for statistical computing. [Internet]. Vienna, Austria: R Foundation for Statistical Computing; 2008. Available from: <http://www.R-project.org>
- 47 . Pagel M. Inferring the historical patterns of biological evolution. *Nature.* 1999 Oct;401(6756):877–84.
- 48 . Blomberg SP, Garland T, Ives AR. Testing for Phylogenetic Signal in Comparative Data: Behavioral Traits Are More Labile. *Evolution.* 2003 Apr;57(4):717–45.
- 49 . Revell LJ. Phytools: An R package for phylogenetic comparative biology (and other things). *Methods Ecol Evol.* 2012;3:217–23.
- 50 . Molina-Venegas R, Moreno-Saiz JC, Castro Parga I, Davies TJ, Peres-Neto PR, Rodríguez MÁ. Assessing among-lineage variability in phylogenetic imputation of functional trait datasets. *Ecography.* 2018;41:1740–9.
- 51 . Akaike H. Information theory and an extension of the maximum likelihood principle. *Second Int Symp Inf Theory.* 1973;267–81.
- 52 . Maddison WP, Maddison DR. Mesquite: a modular system for evolutionary analysis [Internet]. 2018. Available from: <http://www.mesquiteproject.org>
- 53 . Meng J, Hu Y, Li C, Wang Y. The mammal fauna in the Early Cretaceous Jehol Biota: implications for diversity and biology of Mesozoic mammals. *Geol J.* 2006 Sep;41(3–4):439–63.
- 54 . Nowack J, Giroud S, Arnold W, Ruf T. Muscle Non-shivering Thermogenesis and Its Role in the Evolution of Endothermy. *Front Physiol* [Internet]. 2017 Nov 9 [cited 2019 Apr 17];8. Available from: <http://journal.frontiersin.org/article/10.3389/fphys.2017.00889/full>
- 55 . Lowell BB, Spiegelman BM. Towards a molecular understanding of adaptive thermogenesis. *Nature.* 2000 Apr;404(6778):652–60.
- 56 . Hillenius WJ. The evolution of nasal turbinates and mammalian endothermy. *Paleobiology.* 1992;18(01):17–29.
- 57 . Geist NR. Nasal Respiratory Turbinate Function in Birds. *Physiol Biochem Zool.* 2000 Sep;73(5):581–9.
- 58 . Ruben JA. The Evolution of Endothermy in Mammals and Birds: From Physiology to Fossils. *Annu Rev Physiol.* 1995;57:69–95.
- 59 . Crompton AW, Owerkowicz T, Bhullar B-AS, Musinsky C. Structure of the nasal region of non-

- mammalian cynodonts and mammaliaforms: Speculations on the evolution of mammalian endothermy. *J Vertebr Paleontol.* 2017 Jan 2;37(1):e1269116.
- 60 . Lécuyer C, Bogey C, Garcia J-P, Grandjean P, Barrat J-A, Floquet M, et al. Stable isotope composition and rare earth element content of vertebrate remains from the Late Cretaceous of northern Spain (Laño): did the environmental record survive? *Palaeogeogr Palaeoclimatol Palaeoecol.* 2003 May;193(3-4):457-71.
- 61 . Amiot R, Lécuyer C, Buffetaut E, Escarguel G, Fluteau F, Martineau F. Oxygen isotopes from biogenic apatites suggest widespread endothermy in Cretaceous dinosaurs. *Earth Planet Sci Lett.* 2006 Jun 15;246(1-2):41-54.
- 62 . Amiot R, Buffetaut E, Lécuyer C, Wang X, Boudad L, Ding Z, et al. Oxygen isotope evidence for semi-aquatic habits among spinosaurid theropods. *Geology.* 2010 Feb;38(2):139-42.
- 63 . Bernard A, Lécuyer C, Vincent P, Amiot R, Bardet N, Buffetaut E, et al. Regulation of Body Temperature by Some Mesozoic Marine Reptiles. *Science.* 2010 Jun 11;328(5984):1379-82.
- 64 . Haack SC. A thermal model of the sailback pelycosaur. *Paleobiology.* 1986;12(4):450-8.
- 65 . Amprino R. La structure du tissu osseux envisagée comme expression de différences dans la vitesse de l'accroissement. *Arch Biol (Liege).* 1947;58:315-30.
- 66 . de Ricqlès A. Evolution of endothermy: histological evidence. *Evol Theory.* 1974.
- 67 . Chinsamy A, Rubidge BS. Dicyodont (Therapsida) Bone Histology: Phylogenetic and Physiological Implications. *Palaeontol Afr.* 30:1993.
- 68 . Botha J, Chinsamy A. Growth patterns deduced from the bone histology of the cynodonts *Diademodon* and *Cynognathus*. *J Vertebr Paleontol.* 2001;20(4):705-11.
- 69 . Tumarkin-Deratzian AR, Vann DR, Dodson P. Growth and textural ageing in long bones of the American alligator *Alligator mississippiensis* (Crocodylia: Alligatoridae). *Zool J Linn Soc.* 2007 May;150(1):1-39.
- 70 . de Buffrénil V, Castanet J. Age Estimation by Skeletochronology in the Nile Monitor (*Varanus niloticus*), a Highly Exploited Species. *J Herpetol.* 2000 Sep;34(3):414.
- 71 . Castanet J, Curry K, Cubo J, Boisard J-J. Periosteal bone growth rates in extant ratites (ostriche and emu). Implications for assessing. *Comptes Rendus Académie Sci - Ser III - Sci Vie.* 2000;323(6):543-50.
- 72 . De Margerie E, Robin J-P, Verrier D, Cubo J, Groscolas R, Castanet J. Assessing a relationship between bone microstructure and growth rate: a fluorescent labelling study in the king penguin chick (*Aptenodytes patagonicus*). *J Exp Biol.* 2004;207:869-79.
- 73 . Castanet J. Les marques de croissance osseuse comme indicateurs de l'âge chez les lézards. *Acta Zool.* 1978;59:35-48.
- 74 . de Buffrénil V, Mazin J-M. Bone histology of the ichthyosaurs: comparative data and functional interpretation. *Paleobiology.* 1990;16(04):435-47.
- 75 . de Ricqlès AJ, Padian K, Horner JR, Francillon-Vieillot H. Palaeohistology of the bones of pterosaurs (Reptilia: Archosauria): anatomy, ontogeny, and biomechanical implications. *Zool J Linn Soc.* 2000 Jul;129(3):349-85.
- 76 . Houssaye A, Lindgren J, Pellegrini R, Lee AH, Germain D, Polcyn MJ. Microanatomical and Histological Features in the Long Bones of Mosasaurine Mosasaurs (Reptilia, Squamata) – Implications for Aquatic Adaptation and Growth Rates. Farke AA, editor. *PLoS ONE.* 2013 Oct 16;8(10):e76741.
- 77 . Butler RJ, Barrett PM, Gower DJ. Postcranial skeletal pneumaticity and air-sacs in the earliest pterosaurs. *Biol Lett.* 2009 Aug 23;5(4):557-60.
- 78 . Farmer CG, Sanders K. Unidirectional Airflow in the Lungs of Alligators. *Science.* 2010 Jan 15;327(5963):338-40.
- 79 . Huttenlocker AK, Farmer CG. Bone Microvasculature Tracks Red Blood Cell Size Diminution in Triassic Mammal and Dinosaur Forerunners. *Curr Biol.* 2017 Jan;27(1):48-54.

Author contributions

JC designed research; MFB performed histological quantifications, adapted the script from sources and made statistical analyses; JC & MFB wrote the paper

Competing interests

We have no competing interests